Renewable Energy 254 (2025) 123693

Contents lists available at ScienceDirect

Renewable Energy

journal homepage: www.elsevier.com/locate/renene

Integrated membrane gas separation process for the valorisation of H_2 and CO_2 to biomethane

Luigi Marsico [a,b], Adele Brunetti [a,*], Enrico Catizzone [b], Massimo Migliori [b], Giuseppe Barbieri [a]

[a] National Research Council – Institute on Membrane Technology (ITM-CNR), Via Pietro BUCCI, Cubo 17C, Rende CS, 87036, Italy
[b] University of Calabria, Chemical Engineering Catalysis and Sustainable Processes Laboratory, Rende CS, 87036, Italy

A B S T R A C T

In this work, we focused on a membrane gas separation system aimed at enhancing the efficiency of a process for CO_2 valorisation into synthetic methane production via hydrogenation of a biogas stream. This system is designed for separating and recycling unreacted CO_2 and H_2 downstream of a methanation reactor. The inlet stream of the membrane separation system consists of unconverted CO_2 and H_2, apart from the CH_4 from biogas and that produced by CO_2 conversion. The membrane separation is analysed by using performance maps based a 1D mathematical model, already developed and validated, considering the selectivity and permeance properties of a polyimide membrane. The outcomes of the membrane system, constituted by two steps operated at 20 bar, show that the proposed integrated process allows a quantitative CO_2 conversion into methane. The integration of the multi-step membrane process leads to a final retentate stream suitable for direct injection into the gas grid with $CH_4 \geq 97.5$ % molar, and CO_2 and H_2 within the targets of Italian regulation, CH_4 yields up to 0.987 confirmed a nearly complete CO_2 valorisation into CH_4 and a near-zero emissions process.

1. Introduction

Global warming demands the adoption of concrete actions to reduce carbon dioxide emissions and, simultaneously, to develop solutions for its capture and utilization.

Global greenhouse gas emissions reached a historic peak of 57.1 $GtCO_2e$ in 2023, marking an increase of 1.3 % (0.7 $GtCO_2e$) from the preceding year. Fossil CO_2 emissions constitute approximately 68 % of the current greenhouse gas emissions [1] and are predominantly driven by the combustion of coal, oil, and natural gas in the energy sector. Additionally, industrial processes involved in the production of metals, cement, and other materials contribute 9 %, agricultural activities 18 %, and waste management and other sources 4 % [2]. Identifying and promoting alternative and renewable energy sources to replace fossil fuels is then important [3]. To address this challenge, the Intergovernmental Panel on Climate Change has set the target of limiting the increase in global average temperature to 1.5 °C, emphasising the importance of achieving net zero CO_2 emissions by 2050 and deep reductions in emissions of other greenhouse gases, particularly CH_4 [4]. This urgency demands the adoption of innovative strategies aimed at integrating renewable energy production technologies into existing energy systems [5].

Biomethane is one of the potential alternatives to natural gas and can be produced from organic fraction municipal solid waste, sewage sludge, agroforestry residues, via anaerobic digestion process as biogas, a mixture of mainly methane and carbon dioxide [6]. Depending on waste type anaerobic digestion can be carried out in the temperature range 30–45 °C or at a higher temperature of ca. 55 °C where a faster production of biogas can be achieved even if there is a higher energy consumption [7]. It can be used in the markets of energy, heat and transportation [8]. Biogas can be considered a carbon-neutral source of energy or even carbon-negative when considering benefits such as the replacement of fossil fuels but also accounting for the prevention of methane emissions from biomass residues, animal manure, etc. [9]. In 2023, the combined production of biogas and biomethane reached 22 billion cubic meters (bcm), representing 7 % of the European Union's natural gas consumption [10]. Biomethane production alone increased to 4.9 bcm in 2023, with an installed capacity of 6.4 bcm per year anticipated by the first quarter of 2024, demonstrating a notable year-on-year growth of 21 %, concentrated in the EU region. In terms of end uses, 23 % of the biomethane produced in Europe was utilized for transportation, 17 % for building heating, 15 % for power generation, and 13 % for industrial applications. The biogas and biomethane sectors also provide a significant source of biogenic CO_2, a co-product of renewable gas production. Biogenic CO_2 can be harnessed for sustainable production processes, including e-fuels, sustainable chemical

* Corresponding author.
E-mail address: adele.brunetti@cnr.it (A. Brunetti).

https://doi.org/10.1016/j.renene.2025.123693
Received 30 October 2024; Received in revised form 16 April 2025; Accepted 7 June 2025
Available online 13 June 2025

products, and carbon capture and storage. In 2023, Europe had the potential to utilize 29 million tons of biogenic CO_2 based on the volume of biogas and biomethane produced [10].

As mentioned before, biogas typically consists, on dry-basis, of 50–70 % CH_4 and 30–50 % CO_2, along with small amounts of other gases, N_2, O_2, and contaminants, such as H_2S, volatile organic compounds and siloxanes [11]. The production of biomethane suitable for grid injection then requires a biogas upgrading. In this regard, the raw biogas is first purified from contaminants by conventional techniques developed and implemented at industrial scale, such as absorption, adsorption, etc. [12]. Afterwards, the biomethane is retrieved by CH_4/CO_2 separation and the CO_2 is usually released in the atmosphere [13]. Physicochemical methods such as pressure swing adsorption, membranes and absorption with liquid sorbents are in general at high technology readiness levels [14]. Other technologies based on biological processes, classified into chemoautotrophic and photosynthetic are still at an early stage of pilot or full scale implementation [15].

After its separation from CH_4, there is a significant presence of CO_2, which can be utilized as a raw material for producing fuels such as methane or methanol [16]. One of the methods that can be used for the valorisation of CO_2 is its hydrogenation with green hydrogen to methane named the Sabatier reaction (Eq. (1)).

$$CO_2 + 4H_2 \rightleftharpoons CH_4 + 2H_2O \quad (1)$$

$$CO_2 + H_2 \rightleftharpoons CO + H_2O \quad (2)$$

This exothermic reaction (often called carbon dioxide methanation) allows the conversion of CO_2 to CH_4 in the temperature range 300–400 °C and pressures up to 30 bar. Currently, it is considered a suitable way also for the chemical storage of the green H_2 produced from the energy surplus of renewable sources [17]. Interesting estimations reported by Ueckerdt et al. [18], foresee an e-methane cost of about €1200/tCO_2, assuming 100 % renewable energy input, with hypothetical production costs based on large-scale technology projections. The integration of anaerobic digestion with a catalytic unit for converting the CO_2 of the biogas into methane can be then considered not only a strategy to increase the specific methane yield per unit of feedstock but also a route to further improve the contribution of anaerobic digestion in the defossilization strategy, since the CO_2 generated during the process is further valorised into methane to be injected in the gas grid.

The downstream of the methanation reactor mainly contains CH_4 (both bio- and synthetic one), residual unconverted CO_2 and H_2, eventually CO produced as by-product from reverse water gas shift reaction (Eq. (2)) and water vapour. It is then essential to upgrade the methanator downstream to meet the purity target, e.g. for direct injection of CH_4 into the gas grid. Additionally, recovering and recycling back unconverted H_2 and CO_2 to the methanator will increase the methane yield, reducing H_2 losses and CO_2 emission.

The regulations for the injection of methane in the grid are different even within the Countries belonging to the European Union, but as common requirement the content of CH_4 should be always greater than 95 $\%_{molar}$, with a content of H_2 and CO_2 lower than 5 $\%_{molar}$. To treat the downstream of the methanation reactor various operations are proposed such as scrubbers with different absorbent liquid, pressure swing adsorption as well as membrane gas separation [19].

Membranes are valuable for separating gas streams, providing a viable alternative to conventional gas separation technologies [20]. As demonstrated by Collet et al. [21] from an economic point of view, power-to-gas technologies with downstream membrane separation show a higher competitiveness with respect to the amines scrubbing owing to the of the biogas auto-consumption to produce heat for the amines regeneration. Membrane technology is characterised by lower costs, energy consumption, simplicity, and compactness, making it economically and environmentally advantageous [22]. Different membranes can be chosen depending on the species to be separated and the purity and recovery target to be achieved. Despite the trade-off between permeability and selectivity [23], polymeric membranes are currently the most widely used solution at the industrial level [24] owing to their low cost, ease of production, scalability, reproducibility and adaptability. Made of polyimide, polysulfone, polyethersulfone, cellulose acetate, polydimethylsiloxane, polycarbonates, etc., polymeric membranes have been proposed for CO_2 separation from flue gas, biogas upgrading [25] and stream treatments containing hydrogen [26]. Among these, polyimide and cellulose acetate membranes have been mainly used for industrial separation of CO_2/CH_4 [27] and H_2/CH_4 [28]. Overall, in various gas separation applications using membranes, it has been demonstrated that the use of multi-stage membrane systems, properly designed, allows the achievement of purity and recovery goals even with membranes of moderate selectivity. Scholz et al. [29] has demonstrated that in the separation of biogas, the typical trade-off between recovery and purity can be overcome through the implementation of multistage gas permeation networks and that the impact of membrane materials on profitability is not significant if the multistage membrane process is appropriately designed [30]. This approach enables the achievement of both high methane purity and high methane recovery.

Such systems are often necessary when applications require high levels of recovery and purity, which cannot be satisfied using a single-stage [31]. For instance, Evonik Industries has patented a three-stage configuration polyimide-based membrane separation process with a CO_2/CH_4 selectivity of 50, which allows over 99 % CH_4 recovery, with a purity exceeding 96 % molar [32]. Recently, Zito et al. [33], proposed a multistep approach for biogas separation, showing that an increase in the number of steps of a single stage led to significant membrane area savings along with enhanced recovery and purity of the final streams. The use of membrane technology for the treatment of the downstream on methanation reactor has been recently introduced by some authors. Specifically, Gantenbein et al. [34] proposed the use of a membrane gas separation module combining two operational modes for the direct upgrading of biogas to biomethane or for the upgrading of the downstream of a methanator. In contrast, Kirchbacher et al. [19] experimentally analysed the use of thermocatalytical methanation followed by a one-stage gas membrane setup capable of producing high-quality synthetic natural gas. In another work [35], the same authors analysing the economics of four different power-to-gas setups combining catalytic methanation and membrane-based gas upgrading in a context of four different European gas grid standards clearly demonstrated that the CO_2 and H_2 off-gas recycling is a promising option to reduce natural gas and H_2 storage cost. In this work, we designed a membrane gas separation process to enhance the production of methane from the conversion of CO_2 contained in the biogas. The membrane separation process is integrated on the downstream of a methanation reactor, to upgrade the produced methane up to purity levels required for grid injection, recovering, in the meantime, the unconverted CO_2 and H_2 (Fig. 1). The proposed multistage membrane-separation process was designed using performance maps, which provides a quick reference to the effectiveness of each separation step. Each step of the membrane system was properly designed with the aim of maximizing the CH_4 recovery, reducing CO_2 and H_2 losses overall. In all the calculations we assumed the absence of secondary reactions. The outcomes of the membrane system, constituted by two steps operated at 20 bar, were analysed in terms of CO_2 total conversion, CH_4 yield, and membrane area, considering different values of CO_2 conversion in the methanator.

2. Methods

2.1. – The model

The multi-step membrane separation process was designed using performance maps of the concentration versus recovery of the species of interest. These maps were drawn using a 1D mathematical model, already developed and validated [36,37]. All the details about the model are summarised in the Supplementary Information. The model and

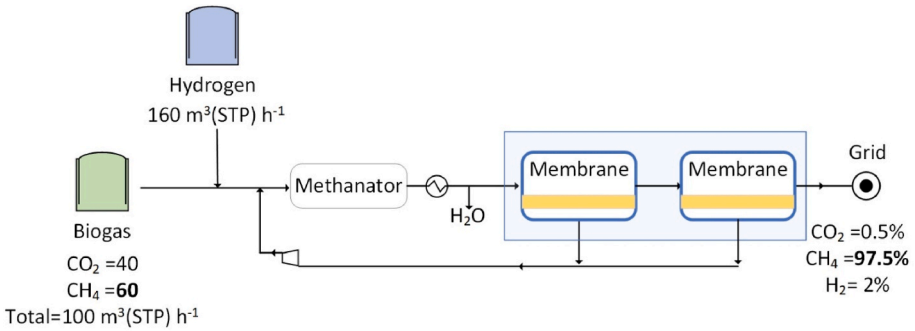

Fig. 1. Scheme of the integrated process.

related simulations provide a quick reference to the effectiveness of each separation step constituting the whole separation process. The inputs of the model are the membrane selectivity and the operating conditions (pressure ratio (Eq. (4)) and feed molar composition of all the species involved). The outputs provide the retentate and permeate flow rates and compositions of the species. Other useful parameters such as retentate composition, permeate composition and membrane area were calculated with a post-processing analysis.

Two main terms of the model can be distinguished:

$$\theta_i = \frac{Permeance_i \, P_i^{Feed} A^{Membrane}}{F_i^{Feed}}, - \tag{3}$$

$$\varphi = \frac{P^{Feed}}{P^{Permeate}}, - \tag{4}$$

The ratio of the maximum flow rate permeating through the membrane and the total flow rate along the module is defined as a permeation number Eq. (3) [36]. Each selected recovery and/or concentration value is associated with a permeation number, from which the membrane area can be immediately calculated for all the membranes with the same selectivity, once the feed pressure and flow rate of the reference species are fixed. The pressure ratio Eq. (4) is the ratio between feed and permeate pressures [36]. The separation performance of the membrane steps was evaluated considering CH_4 recovery in the retentate side Eq. (5) against the molar composition of the single component fed Eq. (6) [38]. The membrane separation properties taken into account are the selectivity, defined as the ratio between the permeances of the two components (Eq. (7)) and the permeance, defined as the ratio of the permeating flux over the transmembrane pressure difference (Eq. (8)) [38].

$$Recovery_{CH_4} = \frac{Flow\ rate_{CH_4}^{Retentate}}{Flow\ rate_{CH_4}^{Feed}}; - \tag{5}$$

$$Molar\ composition_i = \frac{Flow\ rate_i^{Retentate}}{Flow\ rate_{total}^{Retentate}}; - \tag{6}$$

$$Selectivity_{i,j} = \frac{Permeance_i}{Permeance_j}; - \tag{7}$$

$$Permeance_i = \frac{PermeatingFlux_i}{Transmembrane\ Pressure\ Difference_i}; mol\ s^{-1}\ m^{-2}\ Pa^{-1} \tag{8}$$

The capability of the integrated process (i.e., methanation + separation step) to valorise CO_2 into CH_4 was assessed in terms of CH_4 yield as the ratio between the difference of the Outlet/Grid methane flow rate and the one feed to the reactor, divided by the feed carbon dioxide flow rate (Eq. (9)).

$$CH_4\ yield = \frac{Flow\ rate_{CH_4}^{Outlet/Grid} - Flow\ rate_{CH_4}^{Feed}}{Flow\ rate_{CO_2}^{Feed}}, - \tag{9}$$

A unitary yield indicates that the whole CO_2 fed to the process has been valorised into methane, as the stoichiometry of reaction is 1 molecule of CO_2 for 1 molecule of CH_4 (Eq. (1)).

2.2. – The membrane separation properties

Table 1 reports the H_2/CH_4 and CO_2/CH_4 selectivity used as input for the model. To calculate the membrane area required for each step, we considered selectivity and permeance values in line with those generally used for industrial-scale biogas upgrading processes, usually operating at 35–50 °C (Table 1) [39].

2.3. – The performance maps

The performance maps, introduced by Brunetti et al. [36], provide a simple and immediate tool for preliminary analysis of the separation process based on the desired purity and recovery outcomes, considering all membranes with a given selectivity. The maps show the composition of a component as a function of the recovery. The curves on the maps are related to a desired value of selectivity and pressure ratio; each of these curves represents infinitive membrane separation processes, with a process for each point of the curve. A permeation number is associated with each point on the map, from which it is easy to determine, e.g., the membrane area.

Fig. 2 shows an example of performance maps for a feed stream separation composed of 60 % CH_4 and 40 % CO_2. Assuming as an objective the recovery of methane, the less permeable component, it will predominantly be present in the retentate stream. Therefore, performance maps on the retentate side were also developed, showing all the possible compositions of CH_4 and CO_2 as a function of CH_4 recovery.

As a general trend, the molar composition of CH_4 increases as the recovery decreases. For recovery values closer to 1, the CH_4 concentration equals the inlet one because a little separation extent occurred. The composition of CH_4 tends to increase significantly with small reductions in recovery for θ values up to 5. After this point, small increases in the composition correspond to high recovery reductions. Therefore, it is useful to consider concentration and recovery values with θ between 2

Table 1
Properties of polyimide membranes adapted from Ref. [39].

selectivity, -	
H_2/CH_4	90
CO_2/CH_4	45
Permeance, nano-mol s^{-1} m^{-2} Pa^{-1}	
H_2	40
CO_2	20
CH_4	0.44

Table 2
Operating conditions for simulations.

$Flow\ rate^{Feed}_{CO_2}$, m^3(STP) h^{-1}	40
$Flow\ rate^{Feed}_{CH_4}$, m^3(STP) h^{-1}	60
CO_2:CH_4 mixture Feed flow rate, m^3(STP) h^{-1}	100
$Flow\ rate^{Feed}_{H_2}$, m^3(STP) h^{-1}	160
CO_2 methanator conversion, %	60; 70; 80
Membrane separation steps	
P^{Feed}, kPa	2000
$P^{Permeate}$, kPa	100

STP: Standard Temperature and Pressure; 0 °C and 101,325 Pa.

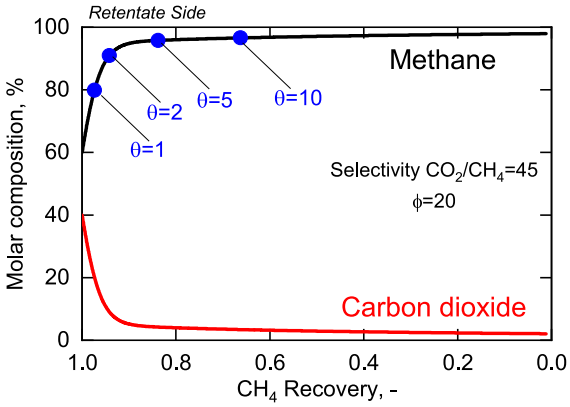

Fig. 2. Performance maps of CH_4 and CO_2 separation.

and 5, to achieve relatively high concentrations and recoveries. Carbon dioxide concentration on the retentate side tends to decrease as the CH_4 retentate recovery decreases because it permeates through the membrane.

2.4. – The operating conditions used in the simulations

In this work, we considered a CO_2:CH_4 mixture with a typical composition of a biogas stream of 40 and 60 % molar, respectively, taking a total volumetric flowrate equals to 100 m^3(STP) h^{-1} as basis for calculations. We assumed a hydrogen stream molar flow rate 4 times that of CO_2 in the biogas feed, according to the stoichiometry of Sabatier reaction. Both biogas and H_2 inlet streams are considered to be at 20 bar, which is the outlet pressure of the methanator, therefore we did not include the compressors on this line. We assumed methane conversion of 60, 70, 80 %, as they are the typical conversion values reported in literature [12]. Furthermore, at temperature lower than 400 °C, Ni-based commercial catalyst, limit the formation of CO via reverse water gas shift reaction (Eq. (2)), and then this compound is not considered in the simulation [40]. In real biogas streams, the presence of components like water and H_2S [41] can impact separation performance, leading to reduced permeability and varied CO_2/CH_4 selectivity. This study focuses on a modelling investigation that uses the mass transport properties of the membrane as input parameters. Permeability and selectivity values used to evaluate separation performance can vary based on the membrane systems, influenced by factors such as operating conditions and feed composition (including the presence of water or impurities). It is crucial to carefully consider these factors when determining the appropriate values for comparing the performance of specific separations, particularly in the presence of contaminants like H_2S, in the proposed results.

Table 2 2 summarizes the operating conditions considered in the simulations.

2.5. – The biomethane recovery and purity targets

As targets of biomethane purity to be achieved by the multi-step membrane process, we considered the Italian legislation for the injection of biomethane into the grid [42,43]. This legislation stipulates that biomethane containing H_2 and CO_2 can be injected into the grid only if the H_2 and CO_2 concentrations are below 2.5 % and 2 % by volume, respectively (Table 3). These maximum values are in line with those of other European countries (France, Sweden, Switzerland, Austria, and the Netherlands) [44] and, in the case of hydrogen, more restrictive. Accordingly, we carried out simulations and designed a multistage membrane process to ensure that the H_2 and CO_2 concentrations remain below this limit, eliminating the need for additional separation of the produced biomethane.

Moreover, as recovery target, it is assumed the constraint of a minimum CH_4 recovery of 90 % of the total amount fed to the process and produced in it.

3. Results and discussion

The multi-step configuration provided valuable insights for designing an adequate process configuration, corresponding to a two-step with recycling of permeate streams of each one, CO_2 and H_2 rich, to the reactor (Fig. 3). This configuration does not require additional compression between the two steps because the first-step retentate flow does not need to be compressed before being fed to the second step. The permeates of both steps (CO_2 and H_2 rich) can be re-compressed and recycled to the reactor, minimizing the H_2 losses and CO_2 emission. To achieve the proposed configuration, performance analyses of single-step and two-step processes were carried out and all details are summarised from Figure S1 to Figure S4 reported in the Supplementary Information. A single stage (Figure S1-Figure S2) was insufficient to reach biomethane composition targets necessary for direct injection into the network. Moreover, the two-step configuration without recycling (Figure S3 and Figure S4) showed high losses of CO_2 (27–72 %) and H_2 (23–62 %) with respect to the feed streams. Stream 5 (Fig. 3) has, thus, a different composition with respect to stream 4, as it accounts for the recycled H_2 and CO_2 from separation stage. Similarly, the simulation assumes that the water is completely removed from biogas before membrane section. Therefore, stream 7 consists of methane, carbon dioxide and hydrogen, only.

Fig. 4 summarizes the performance maps of CH_4, CO_2 and H_2 for the first step (Fig. 4(a) and. 4 (b) and Fig. 4 (c), respectively) and for the second step (Fig. 4(d) and. 4 (e) and Fig. 4 (f), respectively) of the membrane separation process, depicted in Fig. 3, for different CO_2 conversions at the methanation reactor (namely 60 %, 70 % and 80 %). The green areas define the desired recoveries, of at least 90 %, and concentrations, as reported in Table 3.

Starting from the top, the maps show the CH_4, CO_2, and H_2 concentrations in the retentate as a function of CH_4 recovery, for three different values of CO_2 conversion in the methanation reactor.

A high CH_4 recovery corresponds to a lower CH_4 purity, owing to the higher amount of H_2 and CO_2 that remain in the retentate, at all the CO_2 conversion values considered (Fig. 4(a) and. 4 (b), Fig. 4 (c)). The higher the methanator conversion the higher the inlet CH_4 concentration, therefore, the increase in conversion will end with an increase in the amount of CH_4 present in the retentate, at the same recovery. In contrast, the concentrations of CO_2 and H_2 in the retentate decrease when increasing the CO_2 conversion at the methanator, owing to their

Table 3
CO_2 and H_2 concentrations required by Italian regulations for injection into the gas grid [42,43].

H_2 content, %	≤2.0
CO_2 content, %	≤2.5

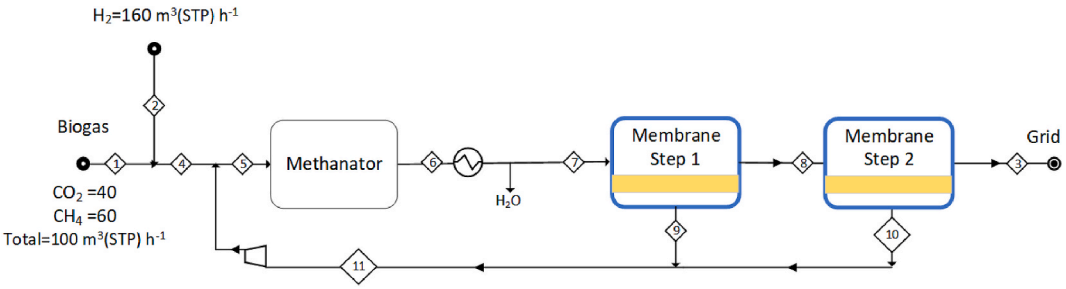

Fig. 3. Integrated process for CO_2 valorisation to methane.

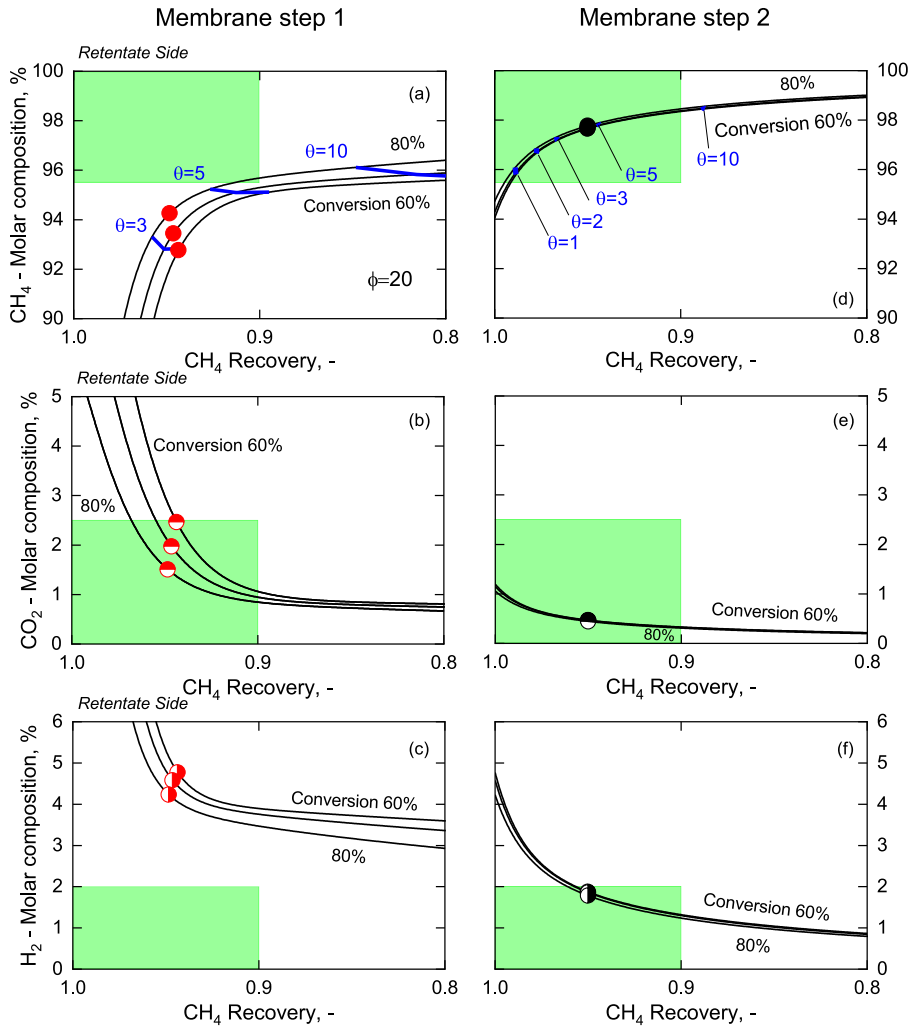

Fig. 4. Retentate performance maps of CH_4, CO_2 and H_2 molar composition (from top to down respectively as a function of CH_4 recovery. Left side – first membrane step separation; Right side – second membrane step separation.

lower concentration in the feed stream to the separation modules. Similar trends are observed for Membrane step 2 (Fig. 4(d) and. 4 (e), Fig. 4 (f)).

The red and half-red circles shown in the map identify the molar composition of CH_4, CO_2 and H_2 respectively in the retentate of the first step, which we selected as the feed conditions to the second one (Fig. 4 (a) and. 4 (b), Fig. 4 (c)). The choice was mainly done to achieve a CH_4 recovery of approximately 95 % on the single step, ensuring an overall recovery of at least 90 % for the entire separation process. For the selected recovery values, θ is between 3 and 5, in dependence of the methanator conversion. The black and half-black circles on the second step maps identify the chosen recoveries and the related molar compositions of CH_4, CO_2 and H_2 respectively in the retentate, which might be fed to the grid, being in the admitted range composition (Fig. 4(d) and. 4 (e), Fig. 4 (f)). Since the most stringent constraint is the hydrogen concentration in the retentate (Table 3), and methane recovery increases with higher hydrogen concentrations, the choice of permeation number values was done considering the maximum allowable hydrogen concentration for grid injection of the retentate stream. This ensured the highest possible methane recovery while maintaining the CO_2 concentration below the regulation limit. In particular, CH_4 is within the acceptable range for all the three methanator conversions considered.

Similarly, CO_2, which reached concentrations below 1 %. Looking at the performance of the entire process, the membrane separation leads to not significant variations in methane recovery, particularly in the concentrations of the output grid-grade stream for each conversion value considered.

The performance of the integrated process is evaluated in terms of CO_2 valorisation expressed in Outlet/Grid methane flow rate. The CH_4 and CO_2 flow rates contained in the biogas and the whole biogas are reported in the figure with red lines (Fig. 5); they represent the input of the integrated process. These two red lines in Fig. 5 – left delineate the range limits of the methane flow rate (named "Outlet/Grid") at the exit of the process. Specifically, when the methane exiting from the integrated process is equal to the whole biogas inlet flow rate, the desired output CH_4 flow rate has been reached, indicating a complete CO_2 valorisation into methane. The lower limit is represented by the methane flow rate in biogas (named "biogas CH_4"), indicating no CO_2 valorisation into methane yet. Overall, the flow rate of methane exiting from the integrated process to be injected into the grid ("Outlet/Grid") is very close to the whole flow rate of biogas fed, indicating a quantitative CO_2 valorisation at the CO_2 conversion considered (Table 4).

Therefore, the membrane separation process allows high CH_4-produced flow rates (difference between CH_4 Outlet/Grid and CH_4 feed flow rates) (Table 4) to be obtained, confirming a quantitative valorisation of CO_2 always higher than 98 %.

The feed flow rate entering the gas separation section, containing CH_4 from biogas, from methanation and the small amount recycled in the permeate, is greater than the whole biogas flow rate owing to the permeates recirculation. Despite the high H_2/CH_4 and CO_2/CH_4 membrane selectivity (Table 1), a small fraction of the CH_4, permeates the membrane and becomes part of the recirculated permeate streams to the methanator. The methanator feed flow is thus greater than the biogas on an additional stream equal to the recirculated one. It can be quantified by the difference between the methanator feed and the lower red line. Looking at the results in terms of CO_2 (Fig. 5 - right side), the red line represents the starting condition, corresponding to the CO_2 contained in the biogas and fed to the process; whereas the "CO_2 desired" condition corresponds to a zero CO_2 flow, which means that the whole CO_2 has been valorised into methane. The exiting CO_2 (Grid/emission) is very close to the desired condition, showing that the membrane process allows the achievement of quantitative CO_2 valorisation. Specifically, CO_2 flow decreases from 40 m^3(STP) h^{-1} at the inlet of the integrated process down to 0.5 m^3(STP) h^{-1} at the exit stream. The CO_2 methanator feed flow rate is much greater than that contained in the biogas (red line) owing to the permeate recycling, which allows the recovery of unreacted reagents (Fig. 5 – right), whereas the membrane stage feed stream will be lower owing to the transformation of reagents. CO_2 streams decrease as the conversion increases owing to the less recycled flow rate (Fig. 5). This reflected in a CH_4 yield always higher than 0.97 (Eq. (9)) showing a quantitative conversion of carbon dioxide into methane, up to 0.987.

Table 4
CH_4 Outlet/Grid flow rate (extracted from Fig. 5), the difference between CH_4 Outlet/Grid and CH_4 feed flow rates and the CH_4 yield of the process as a function of CO_2 methanator conversion.

CO_2 methanator conversion	60 %	70 %	80 %
$Flow\ rate_{CH_4}^{Outlet/Grid}$, m^3(STP) h^{-1}	99.2	99.4	99.5
$Flow\ rate_{CH_4}^{Outlet/Grid} - Flow\ rate_{CH_4}^{Feed}$, m^3(STP) h^{-1}	39.2	39.4	39.5
CH_4 yield of the process	0.979	0.986	0.987

Comparing the results obtained with the regulatory values for CH_4 injection in the grid, it results that for all the considered conditions, the integrated process enables the production of a stream with characteristics suitable for direct injection. Specifically, the allowable inlet grid range for CO_2 concentration is depicted in Fig. 6 with a red area; the maximum regulatory value is 2.5 %. The CO_2 outlet concentration of the membrane separation process, named "CO_2 Grid" and depicted in Fig. 6 with black and white circles, is always well below the maximum value required for grid injection. Therefore, the integrated process allows for a grid fuel stream with a CO_2 concentration well below the maximum permitted value, highlighting the nearly complete valorisation of CO_2 into methane. Consequently, a grid-grade methane stream is achieved, represented in the graph with black circles, exceeding 97 % of methane concentration at every CO_2 conversion considered. This results in a "fuel" concentration, consisting of the sum of CH_4 and H_2 (depicted in

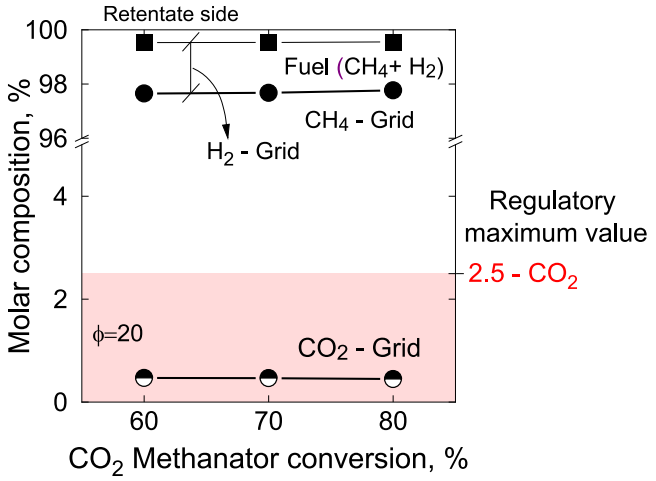

Fig. 6. Membrane section output stream concentration as a function of CO_2 methanator conversion.

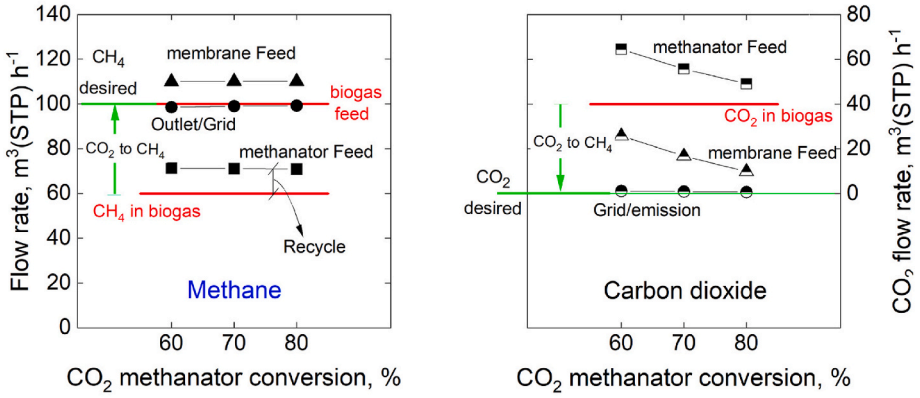

Fig. 5. CH_4 (left) and CO_2 (right) flow rate as a function of CO_2 methanator conversion.

Fig. 6 by squares), always higher than 99 % for all CO_2 conversion considered. The difference between the "fuel" and "CH_4 Grid" represents the hydrogen concentration, which is always lower than the maximum hydrogen regulatory concentration of 2 %.

To further emphasize the competitiveness of the proposed configurations in comparison with those documented in the literature, a comparative analysis was carried out, incorporating results from studies on similar process configurations. Kirchbacher et al. [19] evaluated two process configurations: in the first, the gas mixture consisted exclusively of H_2 and CO_2, while in the second, an additional gas stream derived from fermentation was introduced. In both cases, the gas stream exiting the methanator was treated with polyimide membrane units operating at 14 bar to facilitate CH_4 separation. The results obtained are consistent with those of the present work; however, the higher feed pressure ratio (20 bar) and reactant recycling in the methanator have enabled the achievement of enhanced CH_4 recovery (≥97.9 %) and purity (>97.5 %) (Table 5).

An alternative approach was proposed by Gantenbein et al. [34], who devised a flexible process integrating biogas upgrading and post-upgrading methanation within a single unit, allowing dynamic switching between operational modes. The upgrading was performed using the same membrane system, composed of three counter-current modules: two were utilized in biomethane upgrading mode, whereas three were employed in biogas processing. In the power-to-gas configuration, the authors assumed complete conversion of CO_2 to CH_4, yielding a membrane feed stream containing 12 % H_2 in CH_4. Under these conditions, they successfully reduced the hydrogen concentration below 2 % while operating at a feed pressure between 6 and 8 bar. The presence of CO_2 at varying concentrations in the membrane feed stream, depending on CO_2 conversion efficiency in the methanator, as well as the implementation of a multistage membrane process at 20 bar, are the most significant distinctions between this study and the work of Gantenbein et al. [34], resulting in improved performance even without achieving complete CO_2 conversion in the methanator.

A two-stage membrane process was proposed by Sharifian et al. [45], who carried out a simulation-based study on syngas purification utilizing a combination of a water condenser and hollow-fiber membrane units. In their process scheme, the permeate stream from the first membrane stage was recycled to the reactor, while the permeate from the second stage was redirected to the feed of the first stage. This approach allowed the attainment of 98.2 % CH_4 purity, albeit at a significantly higher operational pressure (50 bar) than that utilized in this study.

In all the aforementioned studies, the focus was predominantly on single-stage or two-stage membrane systems, without a holistic approach toward minimizing CO_2 emissions. This work presents the design of an integrated membrane process consisting of a methanation reactor with different conversions and a multi-step membrane system, all units operating at 20 bar. This configuration incorporates the recycling of permeate streams from the membrane units to maximize CH_4 yield and minimize CO_2 and H_2 losses. The utilization of performance maps facilitated the systematic design of each membrane stage, enabling precise estimation of the membrane area required to meet the specifications for grid injection.

To have an estimation of the variation in membrane areas, we calculated the ratio of the membrane area required at the various methanator conversions compared to the membrane area required when the methanator has a conversion equal to 60 % (Fig. 7). The horizontal line in Fig. 7 shows the level for 60 % CO_2 methanator conversion, serving as a reference for comparison. The values decreased from 0.93 to 0.88 for 70 % and 80 % conversions, respectively. The ratios, and hence the membrane areas, decrease as a consequence of the reduction of the methanator downstream flow rates of unreacted CO_2 and H_2 with increasing conversion. This leads to a smaller membrane area to achieve a grid-grade methane concentration in the outlet stream. Considering the inlet flow rates (Table 2), and the permeance values (Table 1), the calculated membrane area values are reported in Table 6.

Table 5
Comparison with some literature results.

CH_4 recovery, %	CH_4 purity to grid, $\%_{molar}$	H_2 content, $\%_{molar}$	CO_2 content, $\%_{molar}$	Reference
97.9–98.7	>97.5	≤1.9	<0.5	This work
95	>96	<2	<4	[19]
n.a.	>94	<2	<4	[34]
>90	≥97	≤0.5	≤2.5	[35]
n.a.	98.2	1.8	Traces	[45]

4. Conclusions

In this work, we designed a multi-step membrane gas separation system aimed at enhancing the efficiency of a process for CO_2 valorisation into synthetic methane production via hydrogenation of CO_2 contained in a biogas stream. To this purpose, an integrated process consisting of a two-step membrane separation for treating the downstream of a methanator used for converting biogas to methane was proposed. The integrated process allowed the achievement of a CH_4 "Outlet/Grid" stream higher than 99.0 $m^3(STP)h^{-1}$ for CO_2 methanator conversion of 60 %, 70 %, and 80 %, respectively. This value is very close to the whole feed biogas flow rate, indicating quantitative valorisation of CO_2 into CH_4, as confirmed by CH_4 yields of 0.979, 0.986, and 0.987, respectively, as increasing conversion. After the treatment with the membrane process, methane can be directly injected in the grid having a molar concentration always higher than 97.5 % and, CO_2 and H_2 always lower than the regulatory values for grid injection. The permeates of the two membrane steps are recycled back to the methanator, avoiding reactant wastage. Therefore, the proposed configuration effectively addresses the need for CO_2 valorisation into valuable products like CH_4 and promotes the adoption of innovative strategies for integrating renewable energy production technologies into existing energy systems. The proposed integrated scheme is, thus, suitable for existing anaerobic digestion plants for the production of biomethane to be injected in the grid.

CRediT authorship contribution statement

Luigi Marsico: Writing – original draft, Visualization, Investigation, Formal analysis. **Adele Brunetti:** Writing – review & editing,

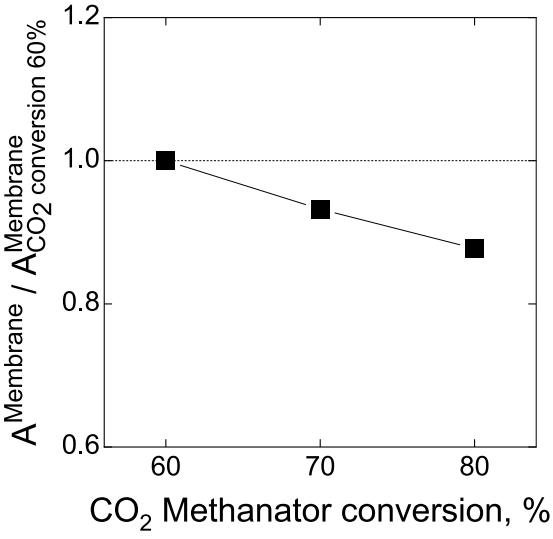

Fig. 7. Membrane area divided by that obtained at 60 % CO_2 conversion (left side) as a function of conversions.

Table 6
Total membrane area at each CO_2 methanator conversion considered.

CO_2 Conversion, %	Total membrane area, m^2
60	191
70	178
80	168

Supervision, Funding acquisition, Formal analysis, Conceptualization. **Enrico Catizzone:** Writing – review & editing. **Massimo Migliori:** Writing – review & editing, Supervision. **Giuseppe Barbieri:** Writing – review & editing, Supervision, Methodology, Investigation, Conceptualization.

Declaration of competing interest

The authors declare that they have no known competing financial interests or personal relationships that could have appeared to influence the work reported in this paper.

Acknowledgements

The authors thank the project "Tech4You—Technologies for climate change adaptation and quality of life improvement"—National Recovery and Resilience Plan (NRRP), Mission 4, Component 2, Investment 1.5, funded from the European Union–NextGenerationEU, Identity code: ECS 00000009, CUP B83C22003980006.

Nomenclature

P	Pressure, Pa
F	flow rate, mol s^{-1}
$A^{membrane}$	membrane Area, m^2
X	molar fraction, -
z	membrane length, m
L	total membrane length, m
Superscripts	
Feed	feed phase referred to
Retentate	retentate phase referred to
Permeate	permeate phase referred to
Outlet/Grid	Outlet/Grid phase referred to
Grid/emission	Grid/emission phase referred to
Subscripts	
i, j	component i and component j of the stream
Greek letters	
θ	permeation number, -
ϕ	pressure ratio, -
Φ	dimensionless flow rate, -
ζ	dimensionless membrane length, -

Appendix A. Supplementary data

Supplementary data to this article can be found online at https://doi.org/10.1016/j.renene.2025.123693.

References

[1] United Nations Environment Programme, Emissions gap report 2024: no more hot air… please! with a massive gap between rhetoric and reality, countries draft new climate commitments. https://wedocs.unep.org/20.500.11822/46404, 2024.
[2] M. Crippa, D. Guizzardi, F. Pagani, M. Banja, M. Muntean, E. Schaaf, F. Monforti-Ferrario, W.E. Becker, R. Quadrelli, A. Risquez Martin, P. Taghavi-Moharamli, J. Köykkä, G. Grassi, S. Rossi, J. Melo, D. Oom, A. Branco, J. San-Miguel, G. Manca, E. Pisoni, , E., P.F. Vignati, GHG Emissions of all World Countries GHG Emissions of all World Countries, Publications Office of the European Union, Luxembourg, 2024, https://doi.org/10.2760/4002897.
[3] IEA (International Energy Agency), Net Zero by (2021) 2050. https://www.iea.org/reports/net-zero-by-2050. (Accessed 16 April 2025).
[4] J. Rogelj, D. Shindell, K. Jiang, S. Fifita, P. Forster, V. Ginzburg, C. Handa, H. Kheshgi, S. Kobayashi, E. Kriegler, L. Mundaca, R. Séférian, M.V. Vilariño, Global warming of 1.5°C. An IPCC special report on the impacts of global warming of 1.5°C above pre-industrial levels and related global greenhouse gas emission pathways, in: The Context of Strengthening the Global Response to the Threat of Climate Change, sustainable development, and efforts to eradicate poverty, 2018, https://doi.org/10.1017/9781009157940.004.
[5] A.T. Hoang, V.V. Pham, X.P. Nguyen, Integrating renewable sources into energy system for smart city as a sagacious strategy towards clean and sustainable process, J. Clean. Prod. 305 (2021) 127161, https://doi.org/10.1016/j.jclepro.2021.127161.
[6] N. Scarlat, J.-F. Dallemand, F. Fahl, Biogas: developments and perspectives in Europe, Renew. Energy 129 (2018) 457–472, https://doi.org/10.1016/j.renene.2018.03.006.
[7] M. Migliori, E. Catizzone, G. Giordano, A. Le Pera, M. Sellaro, A. Lista, G. Zanardi, L. Zoia, Pilot plant data assessment in anaerobic digestion of organic fraction of municipal waste solids, Processes 7 (2019) 54, https://doi.org/10.3390/pr7010054.
[8] O.W. Awe, Y. Zhao, A. Nzihou, D.P. Minh, N. Lyczko, A review of biogas utilisation, purification and upgrading technologies, Waste Biomass Valorization 8 (2017) 267–283, https://doi.org/10.1007/s12649-016-9826-4.
[9] J. Pavičić, K. Novak Mavar, V. Brkić, K. Simon, Biogas and biomethane production and usage: technology development, advantages and challenges in Europe, Energies 15 (2022) 2940, https://doi.org/10.3390/en15082940.
[10] EBA, Statistical Report - Tracking Biogas and Biomethane Deployment Across Europe, 2024. (Accessed 16 April 2025).
[11] E. Santos-Clotas, A. Cabrera-Codony, J. Comas, M.J. Martín, Biogas purification through membrane bioreactors: experimental study on siloxane separation and biodegradation, Separ. Purif. Technol. 238 (2020) 116440, https://doi.org/10.1016/j.seppur.2019.116440.
[12] E. Ryckebosch, M. Drouillon, H. Vervaeren, Techniques for transformation of biogas to biomethane, Biomass Bioenergy 35 (2011) 1633–1645, https://doi.org/10.1016/j.biombioe.2011.02.033.
[13] L. Lombardi, E. Carnevale, Economic evaluations of an innovative biogas upgrading method with CO_2 storage, Energy 62 (2013) 88–94, https://doi.org/10.1016/j.energy.2013.02.066.
[14] Q. Sun, H. Li, J. Yan, L. Liu, Z. Yu, X. Yu, Selection of appropriate biogas upgrading technology-a review of biogas cleaning, upgrading and utilisation, Renew. Sustain. Energy Rev. 51 (2015) 521–532, https://doi.org/10.1016/j.rser.2015.06.029.
[15] I. Angelidaki, L. Treu, P. Tsapekos, G. Luo, S. Campanaro, H. Wenzel, P.G. Kougias, Biogas upgrading and utilization: current status and perspectives, Biotechnol. Adv. 36 (2018) 452–466, https://doi.org/10.1016/j.biotechadv.2018.01.011.
[16] W.Y. Hong, A techno-economic review on carbon capture, utilisation and storage systems for achieving a net-zero CO_2 emissions future, Carbon Capture Sci. Technol. 3 (2022) 100044, https://doi.org/10.1016/j.ccst.2022.100044.
[17] G. Centi, S. Perathoner, The chemical engineering aspects of CO_2 capture, combined with its utilisation, Curr. Opin. Chem. Eng. 39 (2023) 100879, https://doi.org/10.1016/j.coche.2022.100879.

[18] F. Ueckerdt, C. Bauer, A. Dirnaichner, J. Everall, R. Sacchi, G. Luderer, Potential and risks of hydrogen-based e-fuels in climate change mitigation, Nat. Clim. Change 11 (2021) 384–393, https://doi.org/10.1038/s41558-021-01032-7.
[19] F. Kirchbacher, P. Biegger, M. Miltner, M. Lehner, M. Harasek, A new methanation and membrane based power-to-gas process for the direct integration of raw biogas – feasability and comparison, Energy 146 (2018) 34–46, https://doi.org/10.1016/j.energy.2017.05.026.
[20] E. Drioli, G. Barbieri, A. Brunetti, Membrane Engineering for the Treatment of Gases – Volume 1, Royal Society of Chemistry, 2017, https://doi.org/10.1039/9781788010443. ISBN: 978-1-78262-875-0.
[21] P. Collet, E. Flottes, A. Favre, L. Raynal, H. Pierre, S. Capela, C. Peregrina, Techno-economic and life cycle assessment of methane production via biogas upgrading and power to gas technology, Appl. Energy 192 (2017) 282–295.
[22] G. Bernardo, T. Araújo, T. da Silva Lopes, J. Sousa, A. Mendes, Recent advances in membrane technologies for hydrogen purification, Int. J. Hydrogen Energy 45 (2020) 7313–7338, https://doi.org/10.1016/j.ijhydene.2019.06.162.
[23] L.M. Robeson, The upper bound revisited, J. Membr. Sci. 320 (2008) 390–400, https://doi.org/10.1016/j.memsci.2008.04.030.
[24] H.A. Mannan, H. Mukhtar, T. Murugesan, R. Nasir, D.F. Mohshim, A. Mushtaq, Recent applications of polymer blends in gas separation membranes, Chem. Eng. Technol. 36 (2013) 1838–1846, https://doi.org/10.1002/ceat.201300342.
[25] X.Y. Chen, H. Vinh-Thang, A.A. Ramirez, D. Rodrigue, S. Kaliaguine, Membrane gas separation technologies for biogas upgrading, RSC Adv. 5 (2015) 24399–24448, https://doi.org/10.1039/C5RA00666J.
[26] X. Huang, H. Yao, Z. Cheng, Hydrogen separation membranes of polymeric materials, in: Y.P. Chen, S. Bashir, J.L. Liu (Eds.), Nanostructured Materials for Next-Generation Energy Storage and Conversion, Springer, Berlin, Heidelberg, 2017, https://doi.org/10.1007/978-3-662-53514-1_3.
[27] A. Brunetti, G. Barbieri, Membrane engineering for biogas valorization, Front. Chem. Eng. 3 (2021), https://doi.org/10.3389/fceng.2021.775788.
[28] R.W. Baker, Bee ting low, gas separation membrane materials: a perspective, Macromolecules 47 (2014) 6999–7013, https://doi.org/10.1021/ma501488s.
[29] M. Scholz, T. Melin, M. Wessling, Transforming biogas into biomethane using membrane technology, Renew. Sustain. Energy Rev. 17 (2013) 199–212, https://doi.org/10.1016/j.rser.2012.08.009.
[30] M. Scholz, M. Alders, T. Lohaus, M. Wessling, Structural optimization of membrane-based biogas upgrading processes, J. Membr. Sci. 474 (2015) 1–10, https://doi.org/10.1016/j.memsci.2014.08.032.
[31] P.F. Zito, A. Brunetti, E. Drioli, G. Barbieri, CO_2 separation via a DDR membrane: mutual influence of mixed gas permeation, industrial & engineerig, Chem. Res. 59 (2020) 7054–7060, https://doi.org/10.1021/acs.iecr.9b03029.
[32] U.S. Patent Office Confirms Patent Protection for Evonik's 3-stage Process for Efficient Biogas Upgrading with SEPURAN® Green Membranes, 2022.
[33] P.F. Zito, A. Brunetti, G. Barbieri, Multi-step membrane process for biogas upgrading, J. Membr. Sci. 652 (2022) 120454, https://doi.org/10.1016/j.memsci.2022.120454.
[34] A. Gantenbein, J. Witte, S.M.A. Biollaz, O. Kröcher, T.J. Schildhauer, Flexible application of biogas upgrading membranes for hydrogen recycle in power-to-methane processes, Chem. Eng. Sci. 229 (2021) 116012, https://doi.org/10.1016/j.ces.2020.116012.
[35] F. Kirchbacher, M. Miltner, W. Wukovits, M. Harasek, Economic assessment of membrane-based power-to-gas processes for the European biogas market, Renew. Sustain. Energy Rev. 112 (2019) 338–352, https://doi.org/10.1016/j.rser.2019.05.057.
[36] A. Brunetti, F. Scura, G. Barbieri, E. Drioli, Membrane technologies for CO_2 separation, J. Membr. Sci. 359 (2010) 115–125, https://doi.org/10.1016/j.memsci.2009.11.040.
[37] A. Brunetti, E. Drioli, Y.M. Lee, G. Barbieri, Engineering evaluation of CO_2 separation by membrane gas separation systems, J. Membr. Sci. 454 (2014) 305–315, https://doi.org/10.1016/j.memsci.2013.12.037.
[38] R.W. Baker, Membrane Technology and Applications, Wiley, 2004, https://doi.org/10.1002/0470020393.
[39] M. Shahbaz, T. Al-Ansari, M. Aslam, Z. Khan, A. Inayat, M. Athar, S.R. Naqvi, M. A. Ahmed, G. McKay, A state of the art review on biomass processing and conversion technologies to produce hydrogen and its recovery via membrane separation, Int. J. Hydrogen Energy 45 (2020) 15166–15195, https://doi.org/10.1016/j.ijhydene.2020.04.009.
[40] M. Tommasi, S.N. Degerli, G. Ramis, I. Rossetti, Advancements in CO_2 methanation: a comprehensive review of catalysis, reactor design and process optimization, Chem. Eng. Res. Des. 201 (2024) 457–482, https://doi.org/10.1016/j.cherd.2023.11.060.
[41] N. Fajrina, N. Yusof, A.F. Ismail, F. Aziz, M.R. Bilad, M. Alkahtani, A crucial review on the challenges and recent gas membrane development for biogas upgrading, J. Environ. Chem. Eng. 11 (2023) 110235, https://doi.org/10.1016/j.jece.2023.110235.
[42] Ministero dello Sviluppo Economico, Decreto 18-05-2018: Regola Tecnica Sulle Caratteristiche Chimico Fisiche E Sulla Presenza Di Altri Componenti Nel Gas Combustibile, Gazzetta Ufficiale della Repubblica, Italiana, 2018.
[43] Ministero dello Sviluppo Economico, Decreto 03-06-2022: "Aggiornamento Al Decreto Del Ministro Dello Sviluppo Economico Del 18-05-2018".
[44] A. Rafiee, K.R. Khalilpour, J. Prest, I. Skryabin, Biogas as an energy vector, Biomass Bioenergy 144 (2021) 105935, https://doi.org/10.1016/j.biombioe.2020.105935.
[45] S. Sharifian, N. Asasian-Kolur, M. Harasek, Process simulation of syngas purification by gas permeation application, Chem. Eng. Trans. 76 (2019) 829–834.